Pesticide Biochemistry and Physiology 115 (2014) 23–31

Contents lists available at ScienceDirect

Pesticide Biochemistry and Physiology

journal homepage: www.elsevier.com/locate/pest

# Herbicidal effects of harmaline from *Peganum harmala* on photosynthesis of *Chlorella pyrenoidosa*: Probed by chlorophyll fluorescence and thermoluminescence

Chunnuan Deng [a,b], Hua Shao [a], Xiangliang Pan [a,*], Shuzhi Wang [a,c], Daoyong Zhang [a,d]

[a] Laboratory of Environmental Pollution and Bioremediation, Xinjiang Institute of Ecology and Geography, Chinese Academy of Sciences, Urumqi 830011, China
[b] College of Tourism and Geography, Yunnan Normal University, Kunming 650500, China
[c] University of Chinese Academy of Sciences, Beijing 100049, China
[d] State Key Laboratory of Environmental Geochemistry, Institute of Geochemistry, Chinese Academy of Sciences, Guiyang 550002, China

ARTICLE INFO

*Article history:*
Received 17 April 2014
Accepted 12 August 2014
Available online 20 August 2014

*Keywords:*
Phytotoxin
Charge recombination
Photosystem II
$Q_A^-$ reoxidation
Proton gradient
Thermoluminescence

ABSTRACT

The herbicidal effects of harmaline extracted from *Peganum harmala* seed on cell growth and photosynthesis of green algae *Chlorella pyrenoidosa* were investigated using chlorophyll *a* fluorescence and thermoluminescence techniques. Exposure to harmaline inhibited cell growth, pigments contents and oxygen evolution of *C. pyrenoidosa*. Oxygen evolution was more sensitive to harmaline toxicity than cell growth or the whole photosystem II (PSII) activity, maybe it was the first target site of harmaline. The JIP-test parameters showed that harmaline inhibited the donor side of PSII. Harmaline decreased photochemical efficiency and electron transport flow of PSII but increased the energy dissipation. The charge recombination was also affected by harmaline. Amplitude of the fast phase decreased and the slow phase increased at the highest level of harmaline. Electron transfer from $Q_A^-$ to $Q_B$ was inhibited and backward electron transport flow from $Q_A^-$ to oxygen evolution complex was enhanced at 10 μg $mL^{-1}$ harmaline. Exposure to 10 μg $mL^{-1}$ harmaline caused appearance of C band in thermoluminescence. Exposure to 5 μg $mL^{-1}$ harmaline inhibited the formation of proton gradient. The highest concentration of harmaline treatment inhibited $S_3Q_B^-$ charge recombination but promoted formation of $Q_A^-Y_D^+$ charge pairs. *P. harmala* harmaline may be a promising herbicide because of its inhibition of cell growth, pigments synthesis, oxygen evolution and PSII activities.



## 1. Introduction

Allelopathy exists widely in nature. Plant, extracts of plant or plant chemical compounds can produce direct or indirect effect on another plant or microbe by releasing phytotoxins [1,2]. Recently, as an environmentally safe method, allelopathic substances are often suggested as potential natural products to control algal or cyanobacterial blooms in lakes [3]. There is an increasing interest in identifying the allelopathically active macrophyte species as control measures for bloom-forming algae or separating potential natural phytotoxins as effective biological algaecides [4]. Many macrophyte species inhibit growth of cyanobacteria [4,5].

Most allelopathic compounds are more biodegradable and environmentally friendly than traditional herbicides. Some commercial herbicides, such as diuron, atrazine and hexazinone, are photosystem II (PSII) inhibitors by competing with plastoquinone at $Q_B$ binding site of D1 protein in reaction center and inhibiting energy transfer while other herbicides, such as paraquat, act on photosystem I (PSI) [6]. Phytotoxins can produce inhibitory effects as commercial herbicides but may act on different target sites on other plants or algae. Some phytotoxins could influence the growth of neighbor plants or algae [3,7] and change their respiration, photosynthesis, membrane permeability, cell division and development, protein synthesis and enzyme activity [8]. Some phytotoxins directly inhibit photosystem II (PSII) activity, dark respiration and ATP synthesis and induce damage to the antioxidant system [9–11], or inhibit photosynthetic oxygen evolution of intact cyanobacteria, or shift the maximum temperature of the B-band ($S_2Q_B^-$ recombination) to higher temperatures [9], or inhibit the electron transport [11,12].

*Peganum* species distribute wildly in Africa, Middle East, central Asia, South America, Mexico and southern USA [13]. More specifically, the medicinal herb *Peganum harmala* L. is distributed

* Corresponding author. Fax: +86 991 7885446.
*E-mail address:* xiangliangpan@163.com (X. Pan).

http://dx.doi.org/10.1016/j.pestbp.2014.08.002
0048-3575/

throughout northwest China [14] and is used to treat some diseases [15]. Extract of *P. harmala* is phytotoxic, decreases seed germination [16] and inhibits growth of neighboring plants [14]. Alkaloids, such as harmaline, harmine and harmalol, are the main chemical ingredients extracted from *P. harmala*, which are responsible for the antimicrobial, antidepressant and analgesic activities of *P. harmala* [14,17]. Dicot seedling growth is inhibited by 5 μg $mL^{-1}$ harmaline [14]. However, mechanisms of herbicidal effects of harmaline on the physiological processes are still not fully understood. To better understand the effects of harmaline on photosynthesis, its effects on cell growth, electron transport and charge recombination in PSII of the model green algae, *Chlorella pyrenoidosa*, were investigated using *in vivo* chlorophyll fluorescence and thermoluminescence techniques.

Chlorophyll (Chl) *a* fluorescence technique is a sensitive and reliable method to examine the action mode of herbicide on photosynthesis of algae *in vivo* [6,18]. Upon exposure to a strong actinic light, the increase in Chl *a* fluorescence intensity of dark-adapted photosynthetic materials will follow a triphasic kinetic curve starting from its initial level ($F_o$) , two intermediate level ($F_J$ and $F_I$) and to its maximal level ($F_M$ or $F_P$) [19] (called as OJIP). This OJIP curve reflects the successive but overlapping filling-up of photosystem II electron acceptor pools as $Q_A$, $Q_B$ and PQ, whose redox states are controlled by PSII functions [19]. It can be used to analyze changes in electron transfer reaction on both donor and acceptor sides of PSII [20,21]. Based on the OJIP transients, Strasser and his team developed the "JIP" test. The JIP test translates the original data to biophysical parameters that can quantify the energy flow through the reaction center of PSII [22]. The decay of chlorophyll fluorescence (the relaxation kinetics of flash-induced fluorescence) specially provides information of the reoxidation of $Q_A^-$ via forward electron transport to $Q_B$ and back reactions with the $S_2$ state of the oxygen evolving complex [23,24]. Thermoluminescence (TL) is another particular technique to study luminescence, which can reveal different types of charge pairs and subtle changes in charge recombination events in PSII photochemistry [25–27]. In the present study, tests of Chl *a* fluorescence rise transient and relaxation kinetics of flash-induced fluorescence and thermoluminescence techniques were used to probe the targeted action sites of harmaline on electron transport chain in PSII of *C. pyrenoidosa*.

## 2. Materials and methods

### 2.1. Extraction and isolation of harmaline

Three hundred grams of *P. harmaline* seeds were ground into powder and extracted with 500 mL of 80% ethanol [14]. The ethanol extract was concentrated under reduced pressure to yield 52 g of dark red residue which was subsequently dissolved in 200 mL of 5% HCl and filtered. The filtrate was then partitioned three times with 200 mL of chloroform; the chloroform extracts were combined and dried under reduced pressure to give 250 mg of substances, which did not show any major spots on a TLC plate and was then discarded. The aqueous acid layer was made alkaline to pH 9 with $NH_4OH$ and extracted four times with 200 mL of chloroform to yield 8 g of dry chloroform extract. The chloroform extract was then recrystallized in ethanol to give 3.5 g of yellowish crude crystals of total alkaloids. The crystals were further separated on a silica gel column eluted with a step gradient elution (EtOAc/MeOH at 1:0, 98:2, 96:4, 9:1, 8:2, 7:3, 6:4, 1:1, 0:1). Fractions were collected based on TLC profiles and purified to give 140 mg harmaline (detailed method refers to Shao et al. [14]). Structures of compounds were identified by comparing spectral data with published literature [14]. The purified harmaline was used for phytotoxicity test. Harmaline was dissolved in DMSO and diluted to the desired concentrations. 0.1 mL of deionized water or various concentrations of harmaline was added into 20 mL of cell suspension samples to obtain the final nominal harmaline concentrations of 0, 0.5, 1, 5 and 10 μg $mL^{-1}$. The same volume of harmaline-free DMSO solution was used as control.

### 2.2. Culture of C. pyrenoidosa

*C. pyrenoidosa* (FACHB-9) was obtained from the Institute of Hydrobiology, Chinese Academy Sciences. The algae cells were cultivated in BG-11 medium at 25 °C under 30 μmol photons $m^{-2}$ $s^{-1}$ illumination with a 12/12 h light/dark period. Cells in the exponential growth phase were transferred into 50 mL conical flasks for toxicity experiments.

### 2.3. Measurement of cell growth

After exposure to harmaline for 0, 24, 48, and 72 h, the optical density at 680 ($OD_{680}$) of *C. pyrenoidosa* cultures was measured with a UV–vis spectrophotometer (UV2800, Unico, Shanghai, China).

The inhibitory effect ($IC_{50}$) of 72 h treatment of harmaline on the algal growth was estimated from the data that shows a 50% reduction in cell growth of harmaline treated samples compared to control.

### 2.4. Measurement of pigments content

72 h after exposure to harmaline, *C. pyrenoidosa* cells were harvested by centrifugation at 8000 r $min^{-1}$ at 4 °C for 5 min and the pigments were extracted with 96% ethanol for 24 h at 4 °C in the dark followed by centrifugation (8000 r $min^{-1}$, 4 °C, 5 min). Absorption at 470, 649 and 665 nm of the supernatant was measured with the spectrophotometer (UV2800, Unico, Shanghai, China). Chl *a*, Chl *b* and carotenoids contents were calculated [28].

### 2.5. Measurement of oxygen evolution

Oxygen evolution was measured with a Clark-type oxygen electrode (Oxygraph, Hansatech Instruments Ltd., King's Lynn, Norfolk, England). 2 mL of algal cell suspension was added into the reaction cuvette for 5 min oxygen evolution. A white light with illumination on the surface of the cuvette of 150 μmol photons $m^{-2}$ $s^{-1}$ were continuously provided during measurement of $O_2$ evolution (nmol $mL^{-1}$ $min^{-1}$) [29].

### 2.6. Measurement of polyphasic fast fluorescence induction and calculation of JIP test

The polyphasic fast fluorescence induction was performed by using a double-modulation fluorometer (FL3500, PSI, Brno, Czech). The cells used for Chl *a* fluorescence measurements were dark-adapted for 30 min before each test. The polyphasic fluorescence transient was measured with a 1 s multiple turnover flash and recorded every 10 μs for the first 2 ms and every 1 ms up to 1 s [30].

The JIP-test was calculated to analyze each of Chl *a* fluorescence transient [22]. $F_o$ (fluorescence intensity at 50 μs), $F_J$ (fluorescence intensity at around 2 ms) and $F_M$ (maximal fluorescence intensity, usually reached at 200–500 ms) from the original measurements were used. $F_{300\ \mu s}$ are required for calculation of the initial slope ($M_o$) of the relative variable fluorescence ($V$) kinetics. Some selected JIP-test parameters were derived from the fluorescence induction kinetics according to Strasser et al. [31]: $V_j$, relative variable fluorescence at J level; $M_o$, the initial slope, indicating the net

closing rate of the reaction centers; $\Psi_o$, probability that a trapped exciton moves an electron into the electron transport chain beyond $Q_A$ (at $t = 0$); $\varphi_{Po}$, the maximum quantum yield for primary photochemistry (at $t = 0$); $\varphi_{Eo}$, quantum yield of electron transport (at $t = 0$); $\varphi_{Do}$, quantum yield of energy dissipation (at $t = 0$); RC/CS, density of reaction centers; $PI_{ABS}$, photosynthesis performance index on absorption basis; $F_V/F_M$, the maximal PSII photochemical efficiency; ABS/RC, TR/RC, ET/RC and DI/RC, absorption flux, trapped energy flux, electron trans- port flux and dissipated energy flux per reaction center (at $t = 0$), respectively [29].

### 2.7. Measurement of $Q_A^-$ reoxidation kinetics

The relaxation of the flash-induced increase in Chl *a* fluorescence yield reflects the reoxidation of $Q_A^-$ via forward electron transport to $Q_B$ and back reactions with the $S_2$ state of the oxygen evolving complex [23]. The double-modulation fluorometer (FL3500, PSI, Brno, Czech) was also used to measure $Q_A^-$ reoxidation kinetics. The measurement of $Q_A^-$ reoxidation kinetics was performed by a single turnover flash. In this study the $Q_A^-$ reoxidation kinetics curves after a single turnover flash were measured in 400 μs–10 s time range. Both actinic (30 μs) flashes and measuring (2.5 μs) flashes were provided by red LEDs.

### 2.8. Thermoluminescence (TL) measurement

After 6 h of exposure to harmaline, TL measurements of algal cells were performed with the FL2000-S/F thermoluminescence instrument attached to the FL-3500 Double-Modulated Fluorometer (PSI, Brno, Czech). The volume of the samples for each measurement was 0.1 mL. After 5 min of dark adaptation at 25 °C, the cells were cooled to −2 °C and illuminated with one single-turnover flash. Then the cells were warmed up to 65 °C at a heating rate of 0.5 °C $s^{-1}$ and the TL light emission was measured during the heating [26]. For these TL measurements, one single turnover flash was used. Flash dependency of the bands was examined in order to tell the Q band from B band and confirm the AG band. In addition, TL curves for both non-frozen samples (cooling to 1 °C) and in frozen samples (cooling to −5 or −10 °C) and proton gradient were determined to identify the AG band.

### 2.9. Measurement of proton gradient (*ΔpH*)

Transthylakoid proton gradient (ΔpH) and membrane potential ($\Delta\psi$) were measured automatically through extended emitter-detector modules as P515/535 with Dual-PAM-100 system [32]. After longer dark times are given, the P515 displays complex relaxation kinetics for differentiation between $\Delta\psi$ and ΔpH components of the overall proton motive force (pmf) [33]. According to Kramer and Sacksteder [34] the relative amplitudes of $\Delta\psi$ and ΔpH can be estimated from the characteristic levels observed during the light-off response. The difference between the steady state signal and the "dark baseline" reflects $\Delta\psi$ during steady state illumination. The "undershoot" below the "dark baseline" is considered to be a measurement of the steady state of ΔpH. When light is off the accumulated protons are rapidly released from the lumen to the stroma via the ATP-ase, and there is a sudden excess of negative charge at the internal side of the membrane, which results in an inversed P515. Before measurement, samples (control and samples treated with 5 μg $mL^{-1}$ harmaline) were kept for 30 min in darkness. The 550–515 nm signal curves were recorded at dark–light–dark cycle by the Dual-PAM-100 software. The original difference of signals were measured in Volt units, which were transformed into ΔI/I units with the help of the calibration routine. $\Delta\psi$ and ΔpH components of the overall proton motive force (pmf) were calculated in ΔI/I units [32].

### 2.10. Statistics analysis

The experiments were done in triplicate for all treatments. Analysis of the data was done using the software Origin 6.0 (Origin Lab Corporation, USA). The statistical significance between control and harmaline treated samples were calculated in one-way ANOVA (SPSS V16.0) with posthoc Fisher's least significant difference (LSD) test.

## 3. Results

### 3.1. Effect of harmaline on the cell growth

Cell growth of *C. pyrenoidosa* was inhibited by harmaline treatment and the inhibitory effect was dose-dependent (Fig. 1A). After 24 h of exposure to harmaline, there is difference in growth rate between the control and the cells treated with 5 and 10 μg $mL^{-1}$ harmaline. 5 μg $mL^{-1}$ harmaline reduced cell growth by 39% after 24 h of exposure. 72 h after exposure to harmaline, cell growth for 5 and 10 μg $mL^{-1}$ harmaline treatments was reduced by 47% and 55%, respectively in comparison with the control. The 72 h-$IC_{50}$ value was calculated to be 6.7 μg $mL^{-1}$.

### 3.2. Effect of harmaline on $O_2$ evolution

After 6 h of exposure to various concentrations of harmaline, $O_2$ evolution rate of *C. pyrenoidosa* was substantially reduced (Fig. 1B). Treatment with 0.5 and 10 μg $mL^{-1}$ harmaline for 6 h led to a 10% and 47% inhibition of $O_2$ evolution relative to the control.

### 3.3. Effect of harmaline on the content of pigments

Chl *a*, Chl *b* and carotenoids contents decreased as harmaline concentration increased from 1 to 10 μg $mL^{-1}$ (Fig. 1C). For example, Chl *a* content decreased by 15% at 1 μg $mL^{-1}$ harmaline compared to control. Chl *b* content decreased by 47% and 60% at 5 and 10 μg $mL^{-1}$ harmaline, respectively. Carotenoids content decreased by 21% at 1 μg $mL^{-1}$ harmaline and decreased more with elevated harmaline concentration. Chl *a*/*b* ratio was calculated as shown in Fig. 1D. Chl *a*/*b* ratio was not affected at 0–1 μg $mL^{-1}$ harmaline, and had an increase from 1 to 10 μg $mL^{-1}$ harmaline ($p < 0.05$, between 1 and 10 μg $mL^{-1}$ harmaline).

### 3.4. Effect of harmaline on the fast fluorescence rise transient

Effect of harmaline on the fast rise fluorescence transient of *C. pyrenoidosa* was concentration-dependent (Fig. 2A). $F_M$ decreased drastically and the J–P phase leveled off at 5–10 μg $mL^{-1}$ harmaline compared to control, indicating that 5–10 μg $mL^{-1}$ harmaline had strong inhibitory effect on the photochemical activity of *C. pyrenoidosa*. There is no remarkable difference between control and samples treated with 0.5–1 μg $mL^{-1}$ harmaline for JIP-test parameters (Table 1). 5 and 10 μg $mL^{-1}$ harmaline concentration resulted in an increase of $V_j$, $M_o$ and the effective antenna size per reaction center (ABS/RC), and decreased electron transport flux ($\varphi_{Eo}$) and the density of the active photosynthetic reaction centers (RC/CS) (Table 1). These changes resulted in an increase in the dissipated energy flux per reaction center (DI/RC), and finally decreases in the performance index ($PI_{ABS}$) and maximum quantum yield for primary photochemistry ($\varphi_{Po}$, $F_V/F_M$). After exposure to 5 μg $mL^{-1}$ harmaline, $V_j$ (the relative variable fluorescence) and $M_o$ (the initial slope) increased by 24% and 29%, respectively; $\Psi_o$ (probability that a trapped exciton moves an electron into the electron transport chain beyond $Q_A$) and $\varphi_{Eo}$ (quantum yield of electron transport) decreased by 14% and 22%, respectively; $\varphi_{Do}$ (quantum yield of

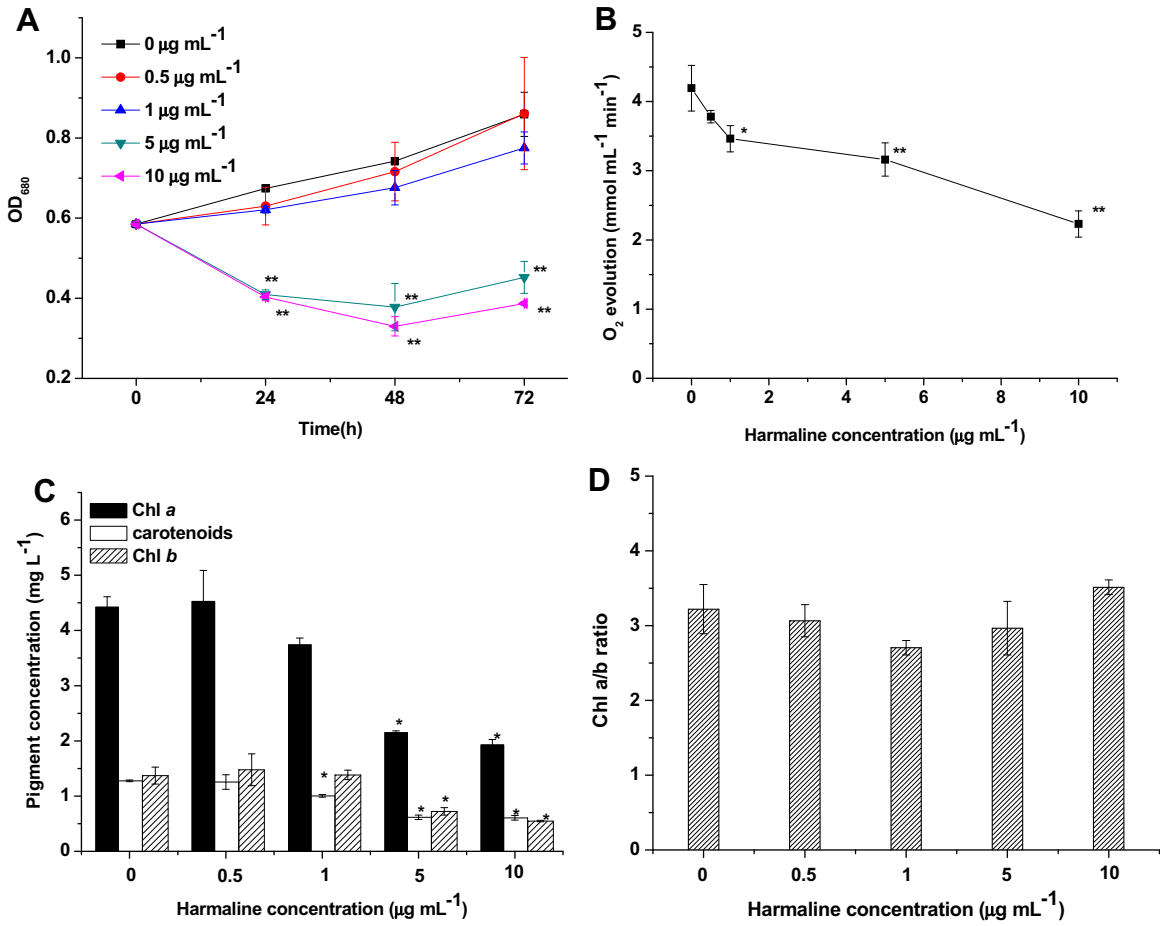


**Fig. 1.** (A) The optical density at 680 nm ($OD_{680}$) of *C. pyrenoidosa* cultures at various concentrations of harmaline after different exposure time. Data were means ± SE ($n = 3$, $^{*}p < 0.05$, $^{**}p < 0.01$). (B) $O_2$ evolution rate of *C. pyrenoidosa* untreated and treated with various concentrations of harmaline for 6 h. Data were means ± SE ($n = 3$). (C) Contents of Chl *a*, Chl *b* and carotenoids of *C. pyrenoidosa* untreated and treated with various concentrations of harmaline for 72 h ($n = 3$). (D) Ratio of Chl *a* and Chl *b* of *C. pyrenoidosa* untreated and treated with various concentrations of harmaline for 72 h ($n = 3$).

energy dissipation) and DI/RC increased by 21% and 38%, respectively; ABS/RC and TR/RC (flux trapped energy flux per reaction center) increased by 14% and 4%, respectively; RC/CS and ET/RC (electron transport flux per reaction center) decreased by 18% and 11%, respectively; and $PI_{ABS}$ and $F_V/F_M$ decreased by 54% and 9%, respectively.

### 3.5. Effect of harmaline on $Q_A^-$ reoxidation

In order to understand the effects of harmaline on the function of the donor side and the acceptor side of PSII, $Q_A^-$ reoxidation kinetics test was performed. The $Q_A^-$ reoxidation kinetic curves of the control and the samples treated with various concentrations of harmaline were shown (Fig. 2B). The curves were fitted by the triexponential equation. The parameters derived from $Q_A^-$ reoxidation kinetic curves were summarized in Table 2. At 0.5–5 μg $mL^{-1}$ harmaline, the fast component dominated the $Q_A^-$ reoxidation kinetics with small fractions of the middle and slow components, and harmaline had little effect on $Q_A^-$ reoxidation kinetics. At 10 μg $mL^{-1}$ harmaline, the fast component decreased to 65.9% while the middle and slow component increased to 23.6% and 10.4%, respectively. Meanwhile, the time constant of fast component slowed from 337 for the control to 986 μs at 10 μg $mL^{-1}$ harmaline.

Thermoluminescence was used to investigate the effect of harmaline on the redox properties of the acceptor and donor sides of PSII, i.e., charge stabilization and subsequent recombination in PSII. TL glow curves were influenced by harmaline (Fig. 3A). The TL curves were well fitted with two or three decomposition components with B1 band ($T_{max}$, the temperature of the maximum, at around 15 °C), B2 band ($T_{max}$ at around 35 °C), and C band ($T_{max}$ at around 62 °C, it only appeared at 10 μg $mL^{-1}$ harmaline) (Fig. 3B). The flash dependency of the TL band at around 15 °C was confirmed to be B1 band by the shift of this band with flash number (Fig. S1). The TL band at 44 °C was not AG band because freezing only increased the thermoluminescence intensity in comparison with unfrozen sample (Fig. S2) and freezing and harmaline treatment both inhibited the formation of proton gradient (Fig. 4).

The peak temperature and intensity were listed in Table 3. B1 band intensity and the $T_{max}$ of B1 band decreased with increasing harmaline concentration. The intensity of B2 band decreased at 5 μg $mL^{-1}$ harmaline. After exposure to 10 μg $mL^{-1}$ harmaline, the C band appeared. The appearances of the C band was accompanied with the decrease of B1 band at 10 μg $mL^{-1}$ harmaline.

### 3.6. Effect of harmaline on the formation of proton gradient

The effect of harmaline on proton gradient was shown in Fig. 4. The proton gradient (ΔpH) was formed for control but its formation was obviously inhibited by 5 μg $mL^{-1}$ harmaline.

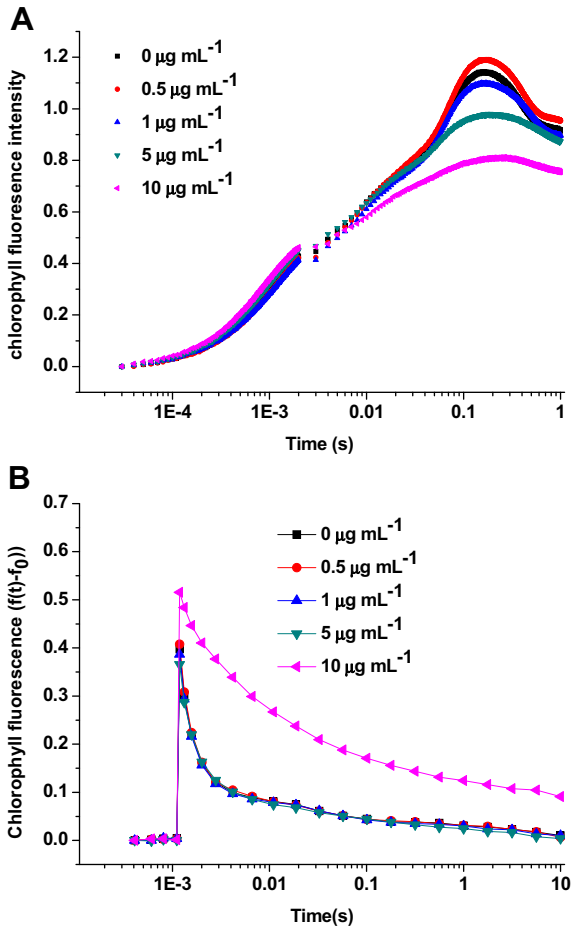


**Fig. 2.** (A) Fast fluorescence rise transient of the control and the samples treated with various concentrations of harmaline for 6 h. Data were means of triplicate. (B) $Q_A^-$ reoxidation kinetic curves of the *C. pyrenoidosa* untreated and treated with various concentrations of harmaline after 6 h exposure time. Data were means of triplicate.

## 4. Discussion

The site of action of harmaline on cell growth, pigments concentration, oxygen evolution and PSII activity of *C. pyrenoidosa* were investigated using *in vivo* Chl *a* fluorescence tests and thermoluminescence techniques.

Cell growth was inhibited by 10–55% after 24 h of exposure to 1–10 μg $mL^{-1}$ harmaline and the strong inhibitory effect remained until 72 h (Fig. 1A). Inhibition of cell growth is usually an important index of many herbicides including some phytotoxins [35,36]. In the present study, 72 h-$IC_{50}$ of harmaline was 6.7 μg $mL^{-1}$, suggesting that harmaline has strong inhibitory effect on green algae compared with other reported herbicides [37].

The contents of Chl *a* and carotenoids were reduced by 1 μg $mL^{-1}$ or higher concentrations of harmaline while Chl *b* content was affected at over 5 μg $mL^{-1}$ harmaline (Fig. 1C). This implies that Chl *a* and carotenoids are more vulnerable to harmaline toxicity than Chl *b*. Reduction of Chl *a* and carotenoids well agreed with other studies [3,35]. The reduction of pigments content observed is most likely due to the reduced biomass of green algae as shown in Fig. 1A. The decrease of Chl *a* after exposure to harmaline indicates a decrease in the antenna size of photosynthetic reaction center complexes [38]. Carotenoids play an important role in non-photochemical quenching (NPQ) and dissipation of excess energy under high light stress to prevent damage to algae

**Table 1**
The selected JIP-test parameters of the control and 6 h of harmaline treated samples. $V_j$, the relative variable fluorescence; $M_o$, the initial slope; $\Psi_o$, probability that a trapped exciton moves an electron into the electron transport chain beyond $Q_A$ (at $t = 0$). $\varphi_{Eo}$, quantum yield of electron transport (at $t = 0$); $\varphi_{Po}$, maximum quantum yield for primary photochemistry (at $t = 0$); $\varphi_{Do}$, quantum yield of energy dissipation (at $t = 0$); $PI_{ABS}$, photosynthesis performance index on absorption basis; $F_v/F_M$, the maximal PSII photochemical efficiency; ABS/RC, TR/RC, ET/RC and DI/RC, absorption flux, trapped energy flux, electron trans- port flux and dissipated energy flux per reaction center (at $t = 0$) respectively; RC/CS, density of reaction centers. $^*p < 0.05$ (LSD test).

| Harmaline (μg $mL^{-1}$) | $V_j$ | $M_o$ | $\Psi_o$ | $\varphi_{Eo}$ | $\varphi_{Do}$ | $PI_{ABS}$ | $F_v/F_M$ | ABS/RC | TR/RC | ET/RC | DI/RC | RC/CS |
|---|---|---|---|---|---|---|---|---|---|---|---|---|
| 0 | 0.37 ± 0.01 | 0.37 ± 0.01 | 0.63 ± 0.01 | 0.44 ± 0.01 | 0.30 ± 0.01 | 2.86 ± 0.28 | 0.71 ± 0.01 | 1.40 ± 0.02 | 0.99 ± 0.02 | 0.62 ± 0.02 | 0.41 ± 0.01 | 1.16 ± 0.01 |
| 0.5 | 0.35 ± 0.00 | 0.33 ± 0.01 | 0.65 ± 0.00 | 0.46 ± 0.00 | 0.29 ± 0.00 | 3.33 ± 0.14 | 0.71 ± 0.00 | 1.32 ± 0.03 | 0.93 ± 0.02 | 0.60 ± 0.01 | 0.39 ± 0.01 | 1.28 ± 0.01 |
| 1 | 0.37 ± 0.00 | 0.37 ± 0.01 | 0.63 ± 0.00 | 0.44 ± 0.01 | 0.30 ± 0.01 | 2.80 ± 0.12 | 0.70 ± 0.01 | 1.40 ± 0.05 | 0.98 ± 0.04 | 0.61 ± 0.03 | 0.42 ± 0.01 | 1.12 ± 0.01 |
| 5 | 0.46 ± 0.02* | 0.48 ± 0.02* | 0.54 ± 0.02* | 0.35 ± 0.02* | 0.36 ± 0.01* | 1.32 ± 0.23* | 0.64 ± 0.01* | 1.60 ± 0.06* | 1.03 ± 0.02 | 0.55 ± 0.00* | 0.57 ± 0.04 | 0.95 ± 0.00 |
| 10 | 0.58 ± 0.01* | 0.65 ± 0.00* | 0.43 ± 0.01* | 0.25 ± 0.01* | 0.41 ± 0.01* | 0.55 ± 0.05* | 0.59 ± 0.01* | 1.92 ± 0.02* | 1.13 ± 0.02* | 0.48 ± 0.02* | 0.79 ± 0.02* | 0.71 ± 0.01* |

**Table 2**
Kinetic deconvolution of $Q_A^-$ reoxidation kinetics of *C. pyrenoidosa* untreated and treated with various concentrations of harmaline ($n = 3$). $A_1$–$A_3$ are the amplitudes; $T_1$–$T_3$ are the time constants.*$p < 0.05$ (LSD test after one way ANOVA).

| Harmaline (μg mL$^{-1}$) | Fast component | | Middle component | | Slow component | |
|---|---|---|---|---|---|---|
| | $A_1$ (%) | $T_1$ (μs) | $A_2$ (%) | $T_2$ (ms) | $A_3$(%) | $T_3$ (s) |
| 0 | 98.4 ± 0.5 | 337 ± 67 | 1.1 ± 0.3 | 13.3 ± 6.1 | 0.4 ± 0.2 | 1.9 ± 0.9 |
| 0.5 | 98.0 ± 0.1 | 393 ± 8 | 1.4 ± 0.1 | 16.7 ± 2.3 | 0.7 ± 0.0 | 3.5 ± 1.0 |
| 1 | 98.3 ± 0.6 | 352 ± 79 | 1.3 ± 0.4 | 15.7 ± 7.2 | 0.5 ± 0.2 | 1.6 ± 0.7 |
| 5 | 96.9 ± 0.5 | 397 ± 47 | 2.2 ± 0.3 | 7.5 ± 3.1 | 1.0 ± 0.2 | 0.6 ± 0.3 |
| 10 | 65.9 ± 1.8* | 986 ± 108* | 23.6 ± 1.2* | 15.9 ± 2.7 | 10.4 ± 0.6* | 0.6 ± 0.2 |

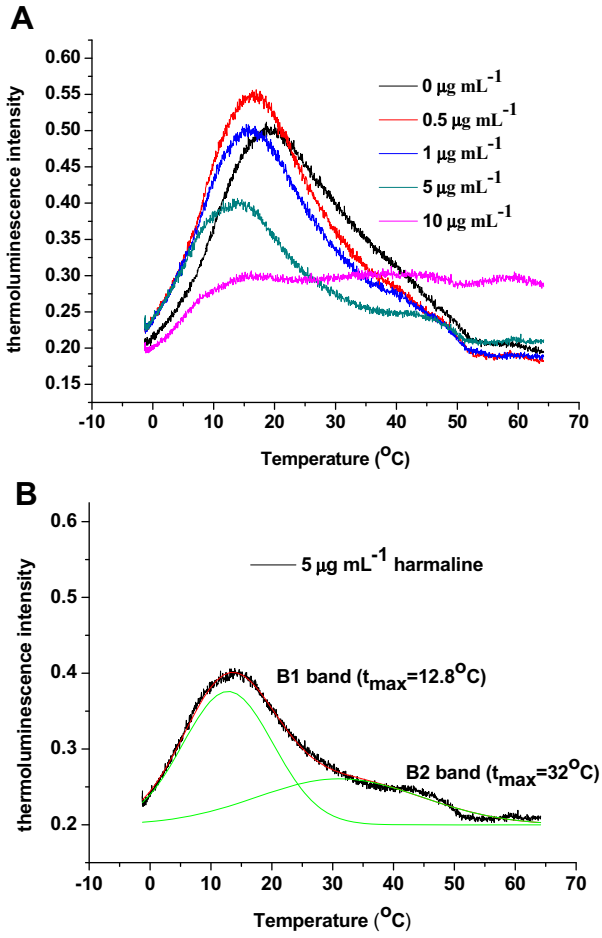


**Fig. 3.** (A) Effect of harmaline on the thermoluminescence (TL) curves of *Chlorella pyrenoidosa* cells untreated and treated with various concentrations of harmaline. Data were means of triplicate. (B) Sample of deconvoluted TL glow curves for algae cells treated with 5 μg mL$^{-1}$ harmaline.

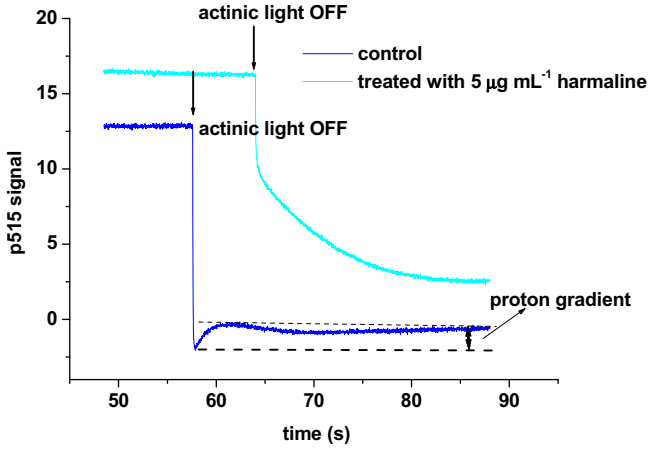


**Fig. 4.** Effect of 5 μg mL$^{-1}$ harmaline on P515 signals. P515 signals were measured as described in Section 2. Samples were illuminated with 126 μmol m$^{-2}$ s$^{-1}$ of photons light and return to darkness.

[39]. Decrease of carotenoids content will decrease oxygen evolution [40] and reduce the dissipation of harmful excess excitation energy [39], which was confirmed by the decreased $O_2$ evolution (Fig. 1B) and increased $\varphi_{Do}$ after exposure to harmaline. Because about 90% of Chl *b* is bound to LHCII (light-harvesting chlorophyll *a*/*b* – protein complex of PSII), the decrease of Chl *b* means the degradation of the LHCII at 5–10 μg mL$^{-1}$ harmaline [41]. Chl *a*/*b* ratio was not affected at 0–1 μg mL$^{-1}$ harmaline but increased at 1–10 μg mL$^{-1}$ harmaline ($p < 0.05$). The increased Chl *a*/*b* ratio indicates that the decrease of Chl *b* content was greater than the decrease of Chl *a* content at 10 μg mL$^{-1}$ harmaline. This suggests that harmaline affects the light-harvesting antenna around PSII and decreases absorption of light energy to avoid more damage from stress.

Oxygen evolution was more sensitive to harmaline toxicity than cell growth, pigments content and PSII activity. For example, the

**Table 3**
Peak temperature and intensity of TL bands in the control and samples treated with various concentrations of harmaline ($n = 3$). The intensities were obtained by calculating the area under the respective peaks. *$p < 0.05$, **$p < 0.01$ (LSD test after one way ANOVA).

| Harmaline | B1 band | | B2 band | | C-band | |
|---|---|---|---|---|---|---|
| (μg mL$^{-1}$) | $T_{max}$ | Intensity | $T_{max}$ | Intensity | $T_{max}$ | Intensity |
| 0 | 18.4 ± 0.6 | 6.78 ± 1.63 | 36.4 ± 1.6 | 2.99 ± 0.92 | – | – |
| 0.5 | 16.3 ± 0.5** | 7.31 ± 0.51 | 35.8 ± 1.3 | 2.40 ± 0.36 | – | – |
| 1 | 15.6 ± 0.3** | 6.40 ± 1.34 | 36.0 ± 1.5 | 2.22 ± 0.28 | – | – |
| 5 | 12.8 ± 0.2** | 3.45 ± 0.64* | 32.0 ± 2.0 | 2.36 ± 0.71 | – | – |
| 10 | 12.29 ± 0.4** | 2.07 ± 0.09** | 39.4 ± 1.6 | 4.63 ± 0.30 | 63.1 ± 0.6 | 2.10 ± 0.61 |

oxygen evolution decreased by 10% compared to control after exposure to 0.5 μg $mL^{-1}$ harmaline for 6 h but cell growth and pigment content were not obviously affected, which was in consistent with some reports about herbicides or other allelochemicals [9]. This implies that photosynthetic apparatus, especially the oxygen-evolving complex, is a very sensitive target site of harmaline exposure. Oxygen evolution is measured with whole cells and a lot of processes influence the activity of oxygen evolution. Effects on fluorescence induction and thermoluminescence were observed at much higher harmaline concentrations. This also indicates that the first target of harmaline may be not the PSII but different sites such as $CO_2$ fixation, the proton gradient and ATP-synthesis.

Electron transfer is usually recognized as a main target of inhibition, which is targeted by many artificial or natural herbicides [9,11]. In the present study, fluorescence transients and the JIP-test parameters changed drastically after exposure to 5–10 μg $mL^{-1}$ harmaline (Table 1), indicating that PSII was an important target of harmaline. The decrease in fluorescence intensities at J–I–P steps were normally explained with the inhibition of the electron transport at the donor side of PSII, which resulted in the accumulation of $P680^+$ [30]. The impacts of harmaline on $O_2$ evolution and Chl *a* also confirmed the inhibitory effects of harmaline on the donor side of PSII. The JIP-test parameters further confirmed that harmaline had inhibitory effects on the donor side of PSII (Table 1). This can be concluded from the decrease in the maximum quantum yield for primary photochemistry ($\varphi_{Po}$) when the cells were treated with 5–10 μg $mL^{-1}$ harmaline. Increase of ABS/RC indicates the change of the antenna size of PSII RC due to the change in the number of LHC complexes per PSII RC or due to the inactivation of RCs and formation of non-$Q_A$ reducing RCs [42]. All these support the fact that harmaline inhibited PSII on the donor side. The decrease of ET/RC showed that harmaline reduced the electron transport of PSII.

The acceptor side of PSII is also the target of various commercial herbicides, and they compete with the native electron acceptor plastoquinone for binding at the $Q_B$ site in the D1 subunit and thus block the electron transfer from $Q_A$ to $Q_B$ [11,43]. The decrease of $\Psi_o$ suggests that the light-independent electron flow from $Q_A^-$ to $Q_B$ was blocked and harmaline might occupy the binding site of $Q_B$ on the reaction center complexes [44]. 5–10 μg $mL^{-1}$ harmaline increased the quantum yield of energy dissipation ($\varphi_{Do}$) and dissipated energy flux (DI/RC), which means that excess excitation energy has been converted to thermal dissipation in order to keep the energy balance between absorption and utilization [29,39]. These changes together caused the drastic decrease of the overall photosynthesis performance index ($PI_{ABS}$).

$Q_A^-$ reoxidation kinetics was done to detect the effects of harmaline on the function of the donor side and acceptor side of PSII of *C. pyrenoidosa*. Three components were identified from the $Q_A^-$ reoxidation kinetics. The fast phase arises from the reoxidation of $Q_A^-$ by PQ9 molecules bound to the $Q_B$ site before the flash [45]. The middle component, originating from $Q_A^-$ reoxidation in centers where the $Q_B$ site was empty at the time of the flash [45], changed considerably with increasing harmaline concentration. The slow phase arises from back reaction of $Q_A^-$ with the $S_2$ state of the water-oxidizing complex, which is populated via the equilibrium between $Q_A^-Q_B$ and $Q_AQ_B^-$. There were a decrease of amplitude of the fast phase and an increase of amplitude of the slow phases at 10 μg $mL^{-1}$ harmaline (Table 2), implying that electron transfer from $Q_A^-$ to $Q_B$ was inhibited by harmaline, more $Q_A^-$ was reoxidized via $S_2(Q_AQ_B)^-$ charge recombination [30,44]. The change may largely be due to modification of the oxygen-evolving complex, especially the alteration of the charge transfer characteristics of the $S_2$ state, which agreed well with the result that oxygen-evolving complex was an important target of harmaline toxicity. The increase of the slow component reflects the fraction of $Q_A^-$ reoxidation through back reactions with the $S_2$ state of the oxygen evolving complex increased after exposure to harmaline. When the $Q_A^-$ to $Q_B$ electron transfer step was inhibited by harmaline, the reoxidation of $Q_A^-$ proceeds via charge recombination with donor side component, mainly with the $S_2$ state, implying that harmaline has similar effect to DCMU. A significant alteration of the decay kinetics was only observed at the highest harmaline concentration. These data indicate again that the first site of inhibition is most likely not PSII.

The proton gradient (ΔpH) component is the key regulatory signal for initiation of nonphotochemical quenching (NPQ) of excitation energy. In the present study, the formation of proton gradient (ΔpH) components of algae cells was inhibited after exposure to 5 μg $mL^{-1}$ harmaline, suggesting that the formation of zeaxanthin was affected under harmaline stress, $H^+$ efflux from the lumen to the stroma via thylakoid ATP-ase was reduced, and the nonphotochemical quenching was influenced. In our previous study, mercury stress decreased the proton gradient of aquatic plant [46]. Increase of energy dissipation in chlorophyll fluorescence test also indicates that nonphotochemical quenching regulation was influenced.

The thermoluminescence technique is also suitable to study the damage to donor and acceptor sides of PSII induced by chemicals [47]. The intensity and position of TL peaks reflect the number and the redox state of the participating charged molecules, respectively [27]. $T_{max}$ of the B1 band is around +20 °C with $S_3Q_B^-$ charge recombination and $T_{max}$ of the B2 band near +30 °C is associated with $S_2Q_B^-$ charge recombination [27]. Exposure to 10 μg $mL^{-1}$ harmaline caused a decrease of B1 band intensity and a slight increase of B2 band intensity (Fig. 3A and Table 3), suggesting that the $S_3Q_B^-$ charge recombination is inhibited but $S_2Q_B^-$ charge recombination is increased after exposure to harmaline. This is different from previous studies. Generally, B band intensity was decreased under environmental stress [48]. Horváth et al. found that $Cu^{2+}$ gradually decreased the intensity of B band with a stepwise shift in its peak position toward the lower temperature [49]. The downshift of B band indicates the inhibition of harmaline of donor side of PSII. The C band with $T_{max}$ at about 50 °C may arise from recombination of the $Q_A^-Y_D^+$ pair [27]. The C band appeared only for samples treated with 10 μg $mL^{-1}$ harmaline. This implies that recombination of the $Q_A^-Y_D^+$ pair was enhanced in the presence of harmaline, which confirmed that the inhibition of harmaline of the acceptor side. It is reported that the intensity of C band is enhanced by high concentration of DCMU [50], which means that harmaline has similar effect.

## 5. Conclusions

Harmaline inhibited cell growth, reduced pigments content, $O_2$ evolution, electron transport on both donor and acceptor sides of PSII of *C. pyrenoidosa*. Oxygen evolution is more sensitive to harmaline toxicity than cell growth or pigment synthesis and it may be the first target site of harmaline. Harmaline exerted influence on the donor side and the acceptor side of PSII. The light-independent electron flow from $Q_A^-$ to $Q_B$ was blocked and harmaline may occupy the binding site of $Q_B$ on the reaction center complexes. Harmaline increased the quantum yield of energy dissipation and reduced the electron transfer in PSII. The charge recombination in PSII was also affected by harmaline which was confirmed by both the $Q_A^-$ reoxidation and thermoluminescence data. The $S_3Q_B^-$ charge recombination was retarded but charge recombinations of $Q_A^-Y_D^+$ pair were promoted at highest concentration of harmaline. *P. harmala* harmaline is a promising herbicide because of its inhibition of cell growth, pigments synthesis, oxygen evolution and PSII activities.

## Acknowledgments

This work was supported by National Natural Science Foundations of China (U1120302 and 21177127). We are grateful to the anonymous reviewers for their valuable comments and suggestions.

## Appendix A. Supplementary data

Supplementary data associated with this article can be found, in the online version, at http://dx.doi.org/10.1016/j.pestbp.2014.08.002.

## References

[1] J.A. Lau, K.P. Puliafico, J.A. Kopshever, H. Steltzer, E.P. Jarvis, M. Schwarzländer, S.Y. Strauss, R.A. Hufbauer, Inference of allelopathy is complicated by effects of activated carbon on plant growth, New Phytol. 178 (2007) 412–423.
[2] C.Y. Yang, S.J. Liu, S.W. Zhou, H.F. Wu, J.B. Yu, C.H. Xia, Allelochemical ethyl 2-methyl acetoacetate (EMA) induces oxidative damage and antioxidant responses in *Phaeodactylum tricornutum*, Pest. Biochem. Phys. 100 (2011) 93–103.
[3] H. Qian, X. Xu, W. Chen, H. Jiang, Y. Jin, W. Liu, Z. Fu, Allelochemical stress causes oxidative damage and inhibition of photosynthesis in *Chlorella vulgaris*, Chemosphere 75 (2009) 368–375.
[4] T.T. Zhang, M. He, A.P. Wu, L.W. Nie, Allelopathic effects of submerged macrophyte *Chara vulgaris* on toxic *Microcystis aeruginosa*, Allelopathy J. 23 (2009) 391–402.
[5] G. Mulderij, B. Mau, E. Van Donk, E.M. Gross, Allelopathic activity of *Stratiotes aloides* on phytoplankton – towards identification of allelopathic substances, Hydrobiologia 584 (2007) 89–100.
[6] F.E. Dayan, M.L.M. Zaccaro, Chlorophyll fluorescence as a marker for herbicide mechanisms of action, Pest. Biochem. Phys. 102 (2012) 189–197.
[7] Y. Hong, H.Y. Hu, F.M. Li, Growth and physiological responses of freshwater green alga *Selenastrum capricornutum* to allelochemical ethyl 2-methyl acetoacetate (EMA) under different initial algal densities, Pest. Biochem. Phys. 90 (2008) 203–212.
[8] T. Haig, Allelochemicals in plants, in: R.S. Zeng, A.U. Mallik, S.M. Luo (Eds.), Allelopathy in Sustainable Agriculture and Forestry, Springer, New York, 2008, pp. 63–104.
[9] E. Leu, A. Krieger-Liszkay, C. Goussias, E.M. Gross, Polyphenolic allelochemicals from the aquatic angiosperm *Myriophyllum spicatum* L. inhibit photosystem II, Plant Physiol. 130 (2002) 2011–2018.
[10] F.E. Dayan, S.O. Duke, Biological activity of allelochemicals, in: A.E. Osbourn, V. Lanzotti (Eds.), Plant-Derived Natural Products: Synthesis, Function and Application, Springer, New York, 2009, pp. 361–384.
[11] J.P. Morrissey, Biological activity of defence-related plant secondary metabolites, in: A.E. Osbourn, V. Lanzotti (Eds.), Plant-Derived Natural Products: Synthesis, Function and Application, Springer, New York, 2009, pp. 283–300.
[12] V.M. Gonzalez, J. Kazimir, C. Nimbal, L.A. Weston, G.M. Cheniae, Inhibition of a photosystem II electron transfer reaction by the natural product sorgoleone, J. Agric. Food Chem. 45 (1997) 1415–1421.
[13] M. Kartal, M.L. Altun, S. Kurucu, HPLC method for the analysis of harmol, harmalol, harmine and harmaline in the seeds of *Peganum harmala* L., J. Pharm. Biomed. Anal. 31 (2003) 263–269.
[14] H. Shao, X.L. Huang, Y.M. Zhang, C. Zhang, Main alkaloids of *Peganum harmala* L. and their different effects on dicot and monocot crops, Molecules 18 (2013) 2623–2634.
[15] A. Astulla, K. Zaima, Y. Matsuno, Y. Hirasawa, W. Ekasari, A. Widyawaruyanti, N.C. Zaini, H. Morita, Alkaloids from the seeds of *Peganum harmala* showing antiplasmodial and vasorelaxant activities, J. Nat. Med. 62 (2008) 470–472.
[16] A.M. Khan, R.A. Qureshi, F. Ullah, S.A. Gilani, Phytotoxic effects of selected medicinal plants collected from Margalla Hills, Islamabad Pakistan, J. Med. Plants Res. 5 (2011) 4671–4675.
[17] H. Berrougui, M. Cordero, A. Khalil, M. Hamamouchia, A. Ettiab, E. Marhuenda, M. Herrara, Vasorelaxant effects of harmine and harmaline extracted from *Peganum harmala* L. seeds in isolated rat aorta, Pharmacol. Res. 54 (2006) 150–157.
[18] D.A. Kopsell, G.R. Armel, K.R. Abney, J.J. Vargas, J.T. Brosnan, D.E. Kopsell, Leaf tissue pigments and chlorophyll fluorescence parameters vary among sweet corn genotypes of differential herbicide sensitivity, Pest. Biochem. Phys. 99 (2011) 194–199.
[19] D. Lazár, The polyphasic chlorophyll a fluorescence rise measured under high intensity of exciting light, Funct. Plant Biol. 33 (2006) 9–30.
[20] I. Rocchetta, H. Küpper, Chromium and copper induced inhibition of photosynthesis in *Euglena gracilis* analysed on the single-cell level by fluorescence kinetic microscopy, New Phytol. 182 (2009) 405–420.
[21] R.J. Strasser, Govindjee, On the O-J-I-P fluorescence transients in leaves and D1 mutants of *Chlamydomonas Reinhardt* II, in: N. Murata (Ed.), Research in Photosynthesis, Kluwer Academic Publishers, Dordrecht, Netherlands, 1992, pp. 23–32.
[22] B.J. Strasser, R.J. Strasser, Measuring fast fluorescence transients to address environmental questions: the JIP-test, in: P. Mathis (Ed.), Photosynthesis: From Light to Biosphere, Kluwer Academic Publishers, Dordrecht, 1995, pp. 977–980.
[23] J. Cao, Govindjee, Chlorophyll a fluorescence transient as an indicator of active and inactive photosystem II in thylakoid membranes, Biochim. Biophys. Acta 1015 (1990) 180–188.
[24] L. Li, X. Chen, D.Y. Zhang, X.L. Pan, Effects of insecticide acetamiprid on photosystem II(PSII) activity of *Synechocystis* sp. (FACHB-898), Pest. Biochem. Phys. 98 (2010) 300–304.
[25] I. Vass, Govindjee, Thermoluminescence from the photosynthetic apparatus, Photosynth. Res. 48 (1996) 117–126.
[26] H.M. Gong, Y.L. Tang, J. Wang, X.G. Wen, L.X. Zhang, C.M. Lu, Characterization of photosystem II in salt-stressed cyanobacterial *Spirulina platensis* cells, Biochim. Biophys. Acta 1777 (2008) 488–495.
[27] P.V. Sane, A.G. Ivanov, G. Őquist, N.P.A. Hüner, Thermoluminescence, in: J.J. Eaton-Rye, B.C. Tripathy, T.D. Sharkey (Eds.), Photosynthesis: Plastid Biology, Energy Conversion and Carbon Assimilation, Advances in Photosynthesis and Respiration 34, Springer Science+Business Media B.V., 2013, pp. 445–474.
[28] H.K. Lichtenthaler, A.R. Wellburn, Determination of total carotenoids and chlorophyll *a* and *b* of leaf extracts in different solvents, Biochem. Soc. Trans. 603 (1983) 591–592.
[29] S.Z. Wang, D.Y. Zhang, X.L. Pan, Effects of arsenic on growth and photosystem II (PSII) activity of *Microcystis aeruginosa*, Ecotoxicol. Environ. Saf. 84 (2012) 104–111.
[30] X.L. Pan, C.N. Deng, D.Y. Zhang, J.L. Wang, G.J. Mu, Toxic effects of amoxicillin on the photosystem II of *Synechocystis* sp. characterized by a variety of *in vivo* chlorophyll fluorescence tests, Aquat. Toxicol. 89 (2008) 207–213.
[31] R.J. Strasser, M. Tsimilli-Michael, A. Srivastava, Analysis of the chlorophyll a fluorescence transient, in: G.C. Papageorgiou, Govindjee (Eds.), Chlorophyll a Fluorescence. A Signature of Photosynthesis. Advances in Photosynthesis and Respiration, Springer, Dordrecht, 2004, pp. 321–362.
[32] U. Schreiber, C. Klughammer, New accessory for the Dual-PAM-100: the P515/535 module and examples of its application, PAM Application Notes 1 (2008) 1–10.
[33] J.A. Cruz, C.A. Sacksteder, A. Kanazawa, D.M. Kramer, Contribution of electric field ($\Delta\psi$) to steady-state transtrylakoid proton motive force(pmf) in *vitro* and in *vivo*. Control of pmf parsing into $\Delta\psi$ and $\Delta$pH by Ionic Strength, Biochemistry 40 (2001) 1226–1237.
[34] D.A. Kramer, C.A. Sacksteder, A diffused-optics flash kinetic spectrophotometer (DOFS) for measurements of absorbance changes in intact plants in the steady-state, Photosynth. Res. 56 (1998) 103–112.
[35] M. Magnusson, K. Heimann, A.P. Negri, Comparative effects of herbicides on photosynthesis and growth of tropical estuarine microalgae, Mar. Pollut. Bull. 56 (2008) 1545–1552.
[36] V. Ebenezer, J.S. Ki, Quantification of toxic effects of the herbicide metolachlor on marine microalgae *Ditylum brightwellii* (Bacillariophyceae), *Prorocentrum minimum* (Dinophyceae) and *Tetraselmis suecica* (Chlorophyceae), J. Microbiol. 51 (2013) 136–139.
[37] J. Ma, L. Xu, S. Wang, R. Zheng, S. Jin, S. Huang, Y. Huang, Toxicity of 40 herbicides to the green alga *Chlorella vulgaris*, Ecotoxicol. Environ. Saf. 51 (2002) 128–132.
[38] O. Björkman, Responses to different quantum flux densities, in: O.L. Lange, P.S. Nobel, C.B. Osmond, H. Ziegler (Eds.), Physiological Plant Ecology I. Encyclopedia of Plant Physiology, Springer-Verlag, Berlin, 1981, pp. 57–107.
[39] P. Müller, X.P. Li, K.K. Niyogi, Non-photochemical quenching. A response to excess light energy, Plant Physiol. 125 (2001) 1558–1566.
[40] K. Dankov, M. Busheva, D. Stefanov, E.L. Apostolova, Relationship between the degree of carotenoid depletion and function of the photosynthetic apparatus, J. Photochem. Photobiol. B: Biol. 96 (2009) 49–56.
[41] Y. Horie, H. Ito, M. Kusaba, A. Tanaka, Participation of chlorophyll *b* reductase in the initial step of the degradation of light-harvesting chlorophyll a/b-protein complexes in *Arabidopsis*, J. Biol. Chem. 284 (2009) 17449–17456.
[42] P. Eullaffroy, C. Frankart, A. Aziz, M. Couderchet, C. Blaise, Energy fluxes and driving forces for photosynthesis in *Lemna minor* exposed to herbicides, Aquat. Bot. 90 (2009) 172–178.
[43] L.W. Hall, J.M. Giddings, K.R. Solomon, R. Balcomb, An ecological risk assessment for the use of Irgarol 1051 as an algaecide for antifoulant paints, Crit. Rev. Toxicol. 29 (1999) 367–437.
[44] X.L. Pan, D.Y. Zhang, X. Chen, G.J. Mu, L.H. Li, A.M. Bao, Effects of levofloxacin hydrochloride on photosystem II activity and heterogeneity of *Synechocystis* sp., Chemosphere 77 (2009) 413–418.
[45] K. Zimmermann, M. Heck, J. Frank, J. Kern, I. Vass, A. Zouni, Herbicide binding and thermal stability of photosystem II isolated from *Thermosynechococcus elongates*, Biochim. Biophys. Acta 1757 (2006) 106–114.
[46] C.N. Deng, D.Y. Zhang, X.L. Pan, F.Q. Chang, S.Z. Wang, Toxic effect of mercury on PSI and PSII activities, membrane potential and transthylakoid proton gradient in *Microsorum pteropus*, J. Photochem. Photobiol. B: Biol. 127 (2013) 1–7.

[47] J. Skotnica, M. Matoušková, J. Nauš, D. Lazár, L. Dvořák, Thermolumnescence and fluorescence study of changes in photosystem II photochemistry in desiccating barley leaves, Photosynth. Res. 65 (2000) 29–40.
[48] N. Mohanty, I. Vass, S. Demeter, Copper toxicity affects photosystem II electron transport at the secondary quinone acceptor $Q_B$, Plant Physiol. 90 (1989) 175–179.
[49] G. Horváth, J.B. Arellano, M. Droppa, M. Barón, Alterations in photosystem II electron transport as revealed by thermoluminescence of Cu-poisoned chloroplasts, Photosynth. Res. 57 (1998) 175–182.
[50] A.N. Misra, F. Dilnawaz, M. Misra, A.K. Biswal, Thermoluminescence in chloroplasts as an indicator of alterations in photosystem 2 reaction centre by biotic and abiotic stresses, Photosynthetica 39 (2001) 1–9.